Title: Direct carbonylation of Glycerol with CO_2 to glycerol carbonate over Zn/Al/La/X (X= F, Cl, Br) Catalysts: the influence of the interlayer anion

Author: Hongguang Li Chunling Xin Xi Jiao Ning Zhao Fukui Xiao Lei Li Wei Wei Yuhan Sun

PII: S1381-1169(15)00116-8
DOI: http://dx.doi.org/doi:10.1016/j.molcata.2015.03.012
Reference: MOLCAA 9451

To appear in: *Journal of Molecular Catalysis A: Chemical*

Received date: 8-10-2014
Revised date: 11-3-2015
Accepted date: 19-3-2015

Please cite this article as: Hongguang Li, Chunling Xin, Xi Jiao, Ning Zhao, Fukui Xiao, Lei Li, Wei Wei, Yuhan Sun, Direct carbonylation of Glycerol with CO2 to glycerol carbonate over Zn/Al/La/X (X= F, Cl, Br) Catalysts: the influence of the interlayer anion, Journal of Molecular Catalysis A: Chemical http://dx.doi.org/10.1016/j.molcata.2015.03.012

Direct carbonylation of Glycerol with CO_2 to glycerol carbonate over Zn/Al/La/X (X= F, Cl, Br) Catalysts: the influence of the interlayer anion

Hongguang Li[a,b], Chunling Xin[a,b], Xi Jiao[a,b], Ning Zhao[a*], Fukui Xiao[a], Lei Li[a], Wei Wei[c], Yuhan Sun[d]

[a] State Key Laboratory of Coal Conversion, Institute of Coal Chemistry, Chinese Academy of Sciences, Taiyuan 030001, China.

[b] University of Chinese Academy of Sciences, Beijing 100049, China.

[c] Center for Greenhouse Gas and Environmental Engineering, Shanghai Advanced Research Institute, Chinese Academy of Sciences, Shanghai, 201210, China.

[d] Low Carbon Conversion Center, Shanghai Advanced Research Institute, Chinese Academy of Sciences, Shanghai 201210, China.

* Corresponding author. Fax: +86-0351-4041153.

E-mail: zhaoning@sxicc.ac.cn (N. Zhao).

Graphic Abstract

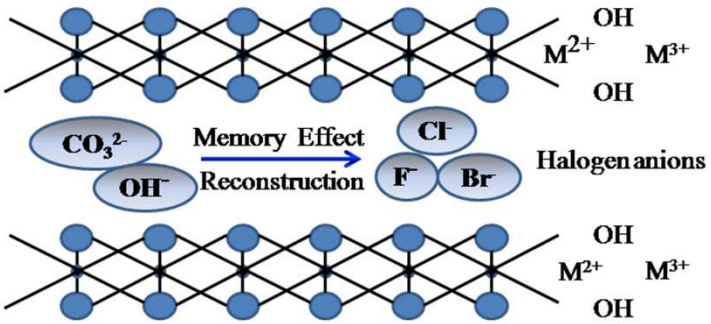

Halogen anions modified Zn/Al/La mixed metal oxides derived form calcination of hydrotalcites shows high catalytic activities for the synthesis of glycerol carbonate form glycerol and CO_2.

Highlights

- The halogen anions enter hydrotalcites follow the sequence of $F^- > Cl^- > Br^-$.
- The basicity decreases with the change of the catalysts' composition.
- The binding energies of Zn $2p_{3/2}$ increase with the introduction of halogen anions.
- The catalytic activity improves by the introduction of halogen anions.

Abstract :

Halogen anions (F^-, Cl^- and Br^-) modified Zn-Al-La (Zn/Al/La=4:1:1) mixed oxides derived from calcination of re-constructed hydrocalcites were prepared and their catalytic activities for the synthesis of glycerol carbonate (GC) form glycerol and CO_2 were investigated. The re-formed hydrotalcites with the introduction of halogen anions formed more thin plates which improved the specific surface area that lead to more exposured active sites. The binding energies of Zn $2p_{3/2}$ increased with the introduction of halogen anions while the basicity decreased with the change of the catalysts' composition. The halogen anions entered hydrotalcites followed the sequence of: $F^- > Cl^- > Br^-$. The halogen anions modified catalysts showed high catalytic activities toward the reaction. The improved catalytic activities were suggested to be closely associated with the structure properties, such as large specific surface area, high surface content of Zn atoms, higher binding energy of Zn $2p_{3/2}$ and high dispersion of metal oxides, which could provide more "accessible" active sites for the reaction. In addition, the changing of halogen anions may also had some influence on the catalytic activity; the introduction of Cl^- had more advantageous for the reaction.

Key words: Glycerol carbonylation; CO_2; ZnAlLa; Halogen anions modified hydrotalcites

1. Introduction

Biodiesel, a renewable clean fuel, has received much attention and as a result, its production increases greatly in recent years[1]. However, a large amount of glycerol, byproduct of biodiesel production, has been produced during the last decade. Excess market-supply of glycerol is not favorable for the development of biodiesel industry[1, 2]. Consequently, new applications for glycerol need to be developed and/or the existing routes need to be expanded. Glycerol carbonate (GC) can be used as a novel component for gas separation membranes, polyurethane foams and surfactant as well as the component in coatings, paints and detergents, etc.[3, 4]. Therefore, the synthesis of glycerol carbonate from glycerol becomes very meaningful.

At present, the main methods for the synthesis of GC form glycerol include the transesterification of glycerol with carbonates, carbonylation of glycerol with urea, direct carbonation of glycerol with CO_2, as well as the reaction of glycerol halo-derivatives with alkaline (hydrogen) carbonates[2, 5]. Transesterification process involves the feed of dimethyl, diethyl or propylene carbonate[6-9], which suffered from the economic disadvantage when compared with urea as feed. Although many heterogeneous catalysts showed good catalytic activity for GC synthesis from glycerol and urea[9-12], the reaction of glycerol with urea must be conducted at the pressure below 20-30 mbar in order to remove the formed ammonia. Moreover, the purification process is also complicated[13].

Compared with the above-mentioned synthesis routes, the direct carbonation of glycerol with CO_2 is a green process that would convert two cheap materials into a valuable product with water as by-product. However, most of catalysts such as zeolites, basic ion-exchange resins, tin complexes, CeO_2-Al_2O_3 and CeO_2-Nb_2O_5 showed low catalytic activities even under high pressure because of the thermodynamic limitation[14-18]. Therefore, acetonitrile was introduced as coupling agent in the process to obtain enhanced results[19], and the catalytic systems of ZnO-$La_2O_2CO_3$ and Cu/La_2O_3 oxides showed enhanced catalytic activities[20, 21]. Although many research works were reported, the development of more efficient solid

catalysts is still a challenge.

It is reported that the mixed metal oxides, derived from calcinations of hydrotalcite-like compounds (HTlcs) ($M^{2+}_{1-x}M^{3+}_{x}(OH)_2^{x+}(A^{n-})_{x/n}\cdot yH_2O$), possess homogeneous dispersion of M^{2+} and M^{3+} with an atomic level, high specific surface area and strongly basic properties. In addition, acid-base properties of the catalysts can be modified by changing cations in the layers, the compensating anions or activation method[22]. As a result, the mixed metal oxides obtained from calcinations of hydrotalcites have been studied for various catalytic reactions including the synthesis of GC by transesterification or carbonylation with urea[6, 9, 23-25].

In our previous research, the effect of Zn:La atomic ratios and calcination temperatures on the activity of glycerol carbonate synthesis were investigated [20]. Therefore, in order to further improve the catalytic performance, the Zn-La containing hydrotalcites (Zn/Al/La=4:1:1) were prepared and tested for the reaction. In addition, for exploration the influence of introduction of different compensating anions on the physico-chemical and catalytic properties, a series of halogen (F, Cl, Br) modified Zn-Al-La (Zn/Al/La=4:1:1) mixed oxides derived from calcinations of re-constructed hydrocalcite compounds were prepared and characterized by XRD, FTIR, TG, BET, XPS, CO_2-TPD. The catalytic activities for the synthesis of GC form glycerol and CO_2 were investigated for the first time. The influence of the halogen anions on physicochemical properties, and the relationship between the catalytic activities and physicochemical properties were discussed.

2. Experimental

2.1. Catalyst preparation

La modified Zn-Al hydrotalcite with the atomic ratio of Zn:Al:La = 4:1:1 were synthesized by co-precipitation method. Typically, two aqueous solutions, a solution of Zn (II), Al (III), La (III) nitrates and a mixed solution of NaOH and Na_2CO_3 precipitant, were added dropwise to 100 mL of deionized water under vigorous stirring with a constant pH of 10. The resulting slurry was aged at 60 ^{o}C for 15 h under stirring and then filtered and washed with deionized water. The obtained solid

were dried at 80 ^{o}C overnight to yield the synthesized hydrotalcite (denoted as HT) and then calcined in air by heating at 5 ^{o}C min^{-1} up to 450 ^{o}C over 5 h under a flowing stream of pure nitrogen to obtain the corresponding mixed oxides (HT-450).

The halogen-containing Zn-Al-La hydrotalcites (HT-X, X= F, Cl, Br) were prepared using the ‘‘memory effect’’ according to the literature[26]. Typically, the as-prepared HT-450 (1.0 g) were treated separately with an aqueous solution of NH_4F (0.1 mol/L, 150 mL) under N_2 atmosphere with stirring at room temperature for 48 h, and the pH values of all solutions were adjusted to 8.0 by addition of appropriate amounts of NH_4OH. Then the resulting products were filtered, washed extensively with deionized water and dried at 80 ^{o}C. The obtained HT-Xs were further calcined at 500 ^{o}C for 5 h under a flowing stream of pure nitrogen and they were denoted as CHT-X. For comparison, Zn-Al-La hydrotalcite was also calcined at 500 ^{o}C and the obtained mixed oxide was denoted as CHT.

2.2. Characterization of Catalysts

X-ray diffraction (XRD) patterns were recorded on a Panalytical X’Pert Pro X-ray diffractometer with Cu Kα radiation over the range of 10–80°. The Fourier Transform Infrared spectra (FT-IR) of the prepared catalysts were obtained using a Nicolet NEXUS 470 FT-IR spectrometer by the KBr disc method over a range of 400–4000 cm^{-1} with a 4 cm^{-1} resolution. The surface area of samples was determined by N_2 adsorption-desorption at liquid nitrogen temperature -196 ^{o}C using a Micromeritics Tristar 3000 instrument. Thermogravimetric analysis (TGA) was performed on Rigaku thermogravimetric analyzer with 60 mL min^{-1} of air flow from 30 to 800 ^{o}C at a heating rate of 10 ^{o}C min^{-1}. The morphology of the samples was performed on a JEOL JSM-7001F scanning electron microscope (SEM) with an accelerating voltage of 10.0 kV.

X-ray photoelectron spectroscopy (XPS) measurements were performed over a Kratos AXIS ULTRA DLD spectrometer equipped with Al Kα radiation (hν = 1486.6 eV) under ultrahigh vacuum. The binding energies were calibrated internally by adventitious carbon deposit C (1s) with E_b = 284.8 eV.

The surface basicity of the catalysts were measured by temperature programmed desorption of CO_2 (CO_2-TPD) and carried out on TPD flow system equipped with an MS detector (Omnistar, PFEIFFER VACUUM). Each sample (0.1 g) was pre-treated in Ar flow at 500 ^oC. The adsorption of CO_2 was performed at 40 ^oC and then followed by Ar purge to remove the physisorbed CO_2. Desorption process was performed at a heating rate of 10 ^oC min-1from 40 ^oC to 500 ^oC.

2.3 Evaluation of Catalysts

The GC synthesis was carried out in a 50 mL stainless-steel autoclave equipped with a magnetic stirrer. In a typical experiment, 4.60 g glycerol, 0.14 g catalyst and 5.0 mL CH_3CN were added into the reactor. Then CO_2 was introduced into the autoclave with an initial pressure of 4.0 MPa. The reaction was conducted at 170 ^oC for 12 h. For quantitative analysis, an external standard-calibration factor method was used and acetonitrile was used as external standard[20]. Considering the low solubility of glycerol and the products in acetonitrile and the high solubility in ethanol, ethanol was also added for the dilution of the reaction mixtures. Qualitative analysis was conducted on a gas chromatograph (FID detector) with a capillary column SHIMADZU CBP/20.

3. Results and discussion

3.1 Textural and structural properties of the prepared materials

The XRD patterns of the prepared precursors are shown in Fig. 1. Besides the typical peaks of HTlcs in HT, the appearance of ZnO and $La_2(CO_3)_2(OH)_2{\cdot}H_2O$ can be ascribed to the high atomic ratio of M^{2+}/M^{3+} (Zn/Al=4) and the large ionic radius of La^{3+}, respectively. Previous reports suggested that the atomic ratio of M^{2+}/M^{3+} between 2 to 4 was favorable for the synthesis of hydrotalcite-like structure[25, 27] and Benito et al. [28] have reported that it was impossible to hinder the ZnO segregation for Zn/Al HTlcs when the Zn^{2+}/Al^{3+} atomic ratio was higher than 2. For HT-450, the hydrotalcite structure collapses and forms the corresponding metal oxide/carbonate. In addition, the original layered structure re-appeares from the

calcined material after rehydration for HT-X while the ZnO peak intensity decreases. The re-appearance of the diffraction peaks of HTlcs in HT-X can be attributed to the "memory effect" of hydrotalcite structure[26]. The weak diffraction peak intensity and the wide peak shape of hydrotalcite in HT-F suggest the re-formed HTlcs with small grain size. Compared with HT, the peak intensity of HTlcs increases for HT-Cl and HT-Br, while decreases for HT-F. HT-Cl has the strongest peak intensity of HTlcs. The results indicate an increasing in crystallinity for HT-Cl and HT-Br which can be ascribed to the Ostwald ripening effect, as described in previous report[25].

It can be seen from Fig. 2 that all the FT-IR spectra are rather similar. The bands at 3435 and 1637 cm^{-1} can be ascribed to the stretching of OH groups attached to metal ions as well as the water molecules in the interlays space[29]. The band at around 1362 cm^{-1} can be attributed to the v_3 mode of interlayer carbonate species, while 1421 cm^{-1} can be assigned to the anti-symmetric stretching mode of the outer layer CO_3^{2-} [27]. It can be found that HT-F shows the lowest peak intensity for interlayer carbonate species (at 1362 cm^{-1}) which can be ascribed to the fact that some parts of CO_3^{2-} was substituted by F^- or OH^-. Previous report described that the anion-exchange selectivity in the HTlcs follows the sequence as: $Br^- < Cl^- < F^- < OH^- < CO_3^{2-}$ [30]. Therefore, compared with HT-F, the increasing of peak intensity for interlayer carbonates species in HT-Cl and HT-Br can be ascribed to the lower anion-exchange ability of Cl^- and Br^- than F^- which lead to a smaller amount of halogen anions (Cl^- and Br^-) entered the interlayer of hydrotalcite. Moreover, the bands at 400-900 cm^{-1} clearly show a typical pattern of hydrotalcite, where strong bands at 615, 552 and 429 cm^{-1} are assigned to the stretching mode of Zn−OH and Al−OH [27, 31], respectively. Compared with HT, the strong peak intensities of Zn−OH and Al−OH in HT-X indicate that more OH^- groups entered the interlayer of hydrotalcite because of the stronger ability of anion-exchange for OH^- than halogen anions.

The scanning electron microscopy images (Fig. 3) shows typical plate-shaped crystals which suggests the formation of layered structure[32]. Compared with HT, the thicknesses of platelets for HT-F are much smaller, indicating that the rebuilding

of the layered structure which is consistent with the result of XRD measurements. In addition, some bulks formed by the growth and/or accumulation of plate-shaped crystals during the process of Ostwald ripening are found in HT-Cl and HT-Br which are accordance with the XRD results (Fig. 1).

Fig. 4 presents the TG-DTG profiles of the precursors. Initially, all the samples behave similarly with respect to the weight loss between 70 to 200 ^{o}C, which corresponds to the removal of physically adsorbed and interlayer water molecules. The removal of both the hydroxyl groups from the HTl network and the carbonate anions from the interlayer are recorded at around 200-300 ^{o}C which results in the formation of corresponding metal carbonate. Finally, the decomposition of metal carbonates formed during the former steps is observed between 300 to 500 ^{o}C, leading to the formation of metal oxide or halide. For HT, the weight loss at around 690 ^{o}C can be ascribed to the decomposition of $La_2O_2CO_3$ [20].

The weight losses of each stage obtained from the TG curves are listed in Table 1. Compared with HT, the weight losses of physically adsorbed and interlayer water increase for HT-X samples, especially for HT-F, which can be ascribed to the formation of more amounts of hydrotalcites (as shown in XRD results, Fig. 1). In addition, the formation of hydrogen bonds between water molecules and interlayer halogen anions also leads to the increasing of the amount of interlayer water. The weight loss of second stage ascribed to the decomposition of hydrotalcites also increases for HT-X samples, especially for HT-Cl, which can be attributed to the re-formation of more hydrotalcites according to the results of XRD and FT-IR. Furthermore, for the decomposition of the formed metal carbonate (third stage), the weight loss decreases for HT-X, especially for HT-Cl, which can be ascribed to the following reasons: firstly, the amount of carbonate species in the interlayer decreases for the re-formed hydrotalcite of HT-X. Moreover, as described in previous report[33], the dehalogenation process seems more difficult than dehydroxylation and decarbonation process which then leads to the decrease of weight loss.

Fig. 5 shows the XRD patterns of the samples after calcination. It is observed that upon thermal decomposition at 500 ^{o}C, the HTl structure collapses and forms the

corresponding metal oxide/carbonate/halide. Some strong diffraction peaks due to ZnO phase appear in all samples. The most obvious difference is the existence forms of La. For CHT and CHT-Br, La exists in the form of $La_2O_2CO_3$ while LaOF and LaOCl become the main phases in CHT-F and CHT-Cl, respectively. The different existence forms of La may have some influence on the surface basicity[34]. In addition, diffraction peaks related to bromide are not found in CHT-Br, indicating that the formed bromide may exist in an amorphous state. Furthermore, compared with CHT, the stronger peak intensity of $La_2O_2CO_3$ indicates $La_2O_2CO_3$ may exist in the form of aggregation in CHT-Br.

The textures of the calcined samples are listed in Table 2. Compared with CHT, the specific surface areas increase significantly from 36.4 to 61.4 m^2 g^{-1} with the introduction of halogen anions. The pore volume and pore radius also increase with the introduction of halogen anions, especially for CHT-Cl. The increasing of specific surface area, pore volume and pore radius for CHT-X can be ascribed to the followed reasons: firstly, the re-formed hydrotalcites with the introduction of halogen anions have more amounts of hydrotalcite structures which results in more amounts of open porous networks after thermal treatment. In addition, compared with HT, the decreasing of the amounts of CO_3^{2-} (2-) leads to a two times of OH^- groups (-) enter the interlayer of halogen anions modified hydrotalcites. Then the dehydroxylation process may result in the formation of more amounts of open-framework structure which is also contributed to the increasing of the surface area, pore volume and pore radius.

The particles of the samples calcined above 500 ^oC maintained morphology similar to that of the precursors, though some crystals were destroyed (Fig. 6). Compared with uncalcined samples (Fig. 3), more homogeneous and thin plates are observed in CHT-X catalysts which can be ascribed to the dehydroxylation and decarbonation during the decomposition process that results in the disappearing of the superimposed bulks, formed during the process of Ostwald ripening. In addition, it can be seen that the thicknesses of plates in CHT-X are much smaller than CHT which is responsible for the increasing of specific surface area for CHT-X (Table 2).

Moreover, compared with CHT, the formed more thin plates in CHT-X improve the metal dispersion which then favors the exposure of more active sites.

3.2 XPS investigations

The calcined samples were analyzed by XPS, and the binding energies (BE) of $Zn2p_{3/2}$, Al2p and La3d are presented in Table 3. For all samples, peaks are found at around 834.4–835.3 eV (BE) for La3d. The $Zn2p_{3/2}$ peak at 1020.8–1021.3 eV can be assigned to the Zn^{2+} species on the catalyst surface. It can be seen that the BE of $Zn2p_{3/2}$ and La3d increase with the introduction of halogen anions, especially for CHT-F. The results can be ascribed to the strong electronegativity of halogen anions which results in more electrons transfer form zinc and lanthanum atoms to halogen atoms. In addition, the formation of LaOF and LaOCl is also favorable for the increase of BE of La atoms. Moreover, the BE of $Zn2p_{3/2}$ and La3d decrease with the change of anions form F^- to Br^- which can be ascribed to the decrease of the electronegativity of Br^-. The high BE of $Zn2p_{3/2}$ in CHT-X can promote the activation of glycerol[20].

Surface compositions of the catalysts, as determined by XPS, are also shown in Table 3. It can be seen that the surface content of Zn^{2+} in CHT-X is higher than that in CHT, which can be related to more amounts of re-formed hydrotalcites in HT-X samples that agree with the results of XRD (Fig. 1) and SEM (Fig. 6). More hydrotalcites improve the surface area (Table 2) and metal dispersion which leads to more amounts of metal active sites exposure on the surface. In addition, the decreasing of surface Zn^{2+} content with the change of halogen anions form F^- to Br^- can be ascribed to the aggregation of ZnO particles which is confirmed by the strong peak intensity of ZnO in CHT-Cl and CHT-Br (Fig. 4). Moreover, the surface content of halogen anions decreases form 4.8 to 0.9% with the anions change from F^- to Br^-. Previous reports described that the anion-exchange selectivity in the HTlcs follows the sequence of: $Br^- < Cl^- < F^-$ [30] and the stability of formed halogen-containing HTlcs also follows the above sequence[35]. Therefore, the decreasing of surface content of halogen anions can be related to the selectivity of anion-exchange and the stability of the re-formed hydrotalcites.

3.3 The basicity of prepared catalysts

The basicity of the catalysts was measured by CO_2-TPD (Fig. 7). According to the previous reports[8, 34], CO_2 desorption peaks can be roughly divided into three regions, e.g. the weakly (50-150 ^oC), moderately (150-400 ^oC) and strongly (> 400 ^oC) basic sites. The weakly basic sites were related to OH^- groups, moderately basic sites were ascribed to metal–oxygen pairs (such as Zn–O, Al–O, and La–O) and strongly basic sites were associated with low-coordination oxygen atoms[34, 36]. All profiles in Fig. 6 can be deconvoluted into four Gaussian peaks assigned to weakly (α peak) and moderately basic sites (β, γ and δ peak), and the peak area can be considered to be the amount of the basic sites. Compared with CHT, the decreasing of α peak area in CHT-X suggests the decrease of the amount of weakly basic sites with the introduction of halogen anions which is in accordance with the result of previous reports[25, 37]. In addition, the total peak area of the sum of β, γ and δ decrease for CHT-X catalysts, especially for CHT-Cl, which indicates the decrease of the amount of moderately basic sites. The phenomenon can be explained as follows:

The more amounts of moderately basic sites in CHT can be related to the formation of $La_2O_2CO_3$. Previous reports described that the introduction of La may enhance the basicity of catalysts[38] via the formation of $La_2O_2CO_3$ [39]. However, although CHT-X shows large surface area, the amount of moderately basic sites in CHT-X decreases which suggests that the amount of basic sites is not only correlated to the surface area of the catalysts [20, 36]. In addition, as shown in Fig. 4, the existence forms of La changes with the introduction of halogen anions which may have some influence on the surface basicity[34]. Therefore, the formation of LaOF and LaOCl may be responsible for the reduction of the amount of moderately basic sites. For CHT-Br, the decrease of the amount of moderately basic site may be related to the aggregation of $La_2O_2CO_3$ (Fig. 5). Moreover, the formed amorphous bromide may also account for the decreasing of the amount of moderately basic site for CHT-Br.

3.4 Catalytic activity

The catalytic performances for GC synthesis of the prepared catalysts are

summarized in Table 4. The reaction conditions are similar with the previous report[20]. Acetonitrile was employed since previous reports suggested that acetonitrile is an effective coupling agent for the process[19]. However, monoacetin and diacetin are also detected as by-products which result from the reaction of glycerol and acetic acid derived from hydrolysis of acetonitrile[20]. Although the formation of acetins as byproducts cannot be avoided, the wide applications of the byproducts may reduce the cost of the synthesis route, e.g. monoacetin can be used in the manufacture of dynamite and tanning leather, as a solvent for various dyes, as food additive, plasticisers and softening agents. While diacetin can be used as solvent, softening agent and fuel additives for viscosity reduction[40, 41].

Compared with CHT, the catalytic activities are improved with the introduction of halogen anions. A maximum glycerol conversion of 35.5% with GC yield of 16.0% is obtained over CHT-Cl. In addition, the higher selectivity towards acetins than GC can be ascribed to the impurity of glycerol and acetonitrile which were analytical agents and the fact that there was no dehydration processing. Similar results were obtained in previous report[42]. Furthermore, the selectivity toward GC increases with the introduction of halogen anions. The improvement of the catalytic activities with the introduction of halogen anions can be speculated from the catalyst characteristics.

The increasing of diffraction peak intensity of hydrotalcite in the halogen anions modified samples (Fig. 1) indicates that more amounts of hydrotalcites were formed which enhances the dispersion of active components and then improves the catalytic activities. In association with the result of the N_2 adsorption, the introduction of halogen anions improves the specific surface area (Table 2) which favors the exposure of more active sites. In addition, the SEM images shown in Fig. 5 also suggest that the formed thin plates in CHT-X favors the enhancement of the dispersion and exposure of active sites. Furthermore, considering the results of XPS, the increasing of the BE of $Zn2p_{3/2}$ in CHT-X favors the activation of glycerol[20], and the increasing of the surface Zn content in CHT-X is also helpful to improve the glycerol activation.

Previous reports described that moderately basic sites is favorable for the

synthesis of GC from glycerol and CO_2, due to the strong ability of moderately basic sites for the activation of CO_2 and hydrolysis of acetonitrile[20, 43]. In our experiments, although the amounts of moderately basic sites decrease for CHT-X (Fig. 6), the increasing of the catalytic activities may indicate that the amount of moderately basic sites is not the key factor for catalytic activity. The decreasing of the amount of moderately basic sites may not favorable for acetonitrile hydrolysis which may results in the decreasing of the formation of acetins and the increasing of the selectivity of GC.

The improvement of the catalytic activities for CHT-X may also be associated with the halogen anions. Previous research results suggested that different anions had great influence on the catalytic activities and the introduction of Cl^- and Br^- obviously improved the catalytic activities[44]. In addition, Park et al. have reported that the Cl^- could be considered as Lewis base to activate glycerol[45]. Therefore, the improvement of the catalytic activities may be related to the halogen anions which may activate glycerol.

The stability of CHT-Cl was investigated and the result is shown in Table 4. It can be found that the glycerol conversion and GC yield decrease which can be ascribed to the loss of the active component (such as Zn^{2+} and Cl^-) by leaching[12, 46]. In addition, the selectivity of GC increases from 45.2% to 52.3%, which can be attributed to the existence of zinc glycerolate on the surface of the used catalyst as described in our previous report[46]. The result indicates that the stability of the halogen anions modified catalysts is not good, it is necessary to develop highly efficient and stable catalyst.

4. Conclusion

Halogen anions (F^-, Cl^-, Br^-) modified Zn/Al/La catalysts derived from hydrotalcite-like compounds were prepared and tested for glycerol carbonate synthesis from glycerol carbonylation with CO_2. It is found that the introduction of halogen anions has significant influence on the physicochemical and catalytic properties of the Zn/Al/La catalysts. The following conclusions may be drawn:

(1) The specific surface area increase with the introduction F^-, Cl^- and Br^- anions. The binding energy of $Zn2p_{3/2}$ increase for the halogen anions modified samples, while the catalyst basicity decreases with the formation of LaOF and LaOCl. In addition, the ability of halogen anions enter the hydrotalcite structure follows the sequence of: $Br^- < Cl^- < F^-$.

(2) The catalytic activity is improved with the introduction of halogen anions, and the best catalytic performance is obtained on CHT-Cl.

(3) The catalytic activity may associate with the specific surface area, surface content of Zn as well as binding energy of Zn atoms. The surface basicity has some influence on the selectivity of glycerol carbonate. In addition, the halogen anions also have great influence on the catalytic activities.

Acknowledgements

This work was financially supported by National Natural Science Foundation of China (21306217).

Reference

[1] J.M. Clomburg, R. Gonzalez, Trends in biotechnol. 31 (2013) 20-28.

[2] C.H. Zhou, H. Zhao, D.S. Tong, L.M. Wu, W.H. Yu, Catal. Rev. 55 (2013) 369-453.

[3] M.O. Sonnati, S. Amigoni, E.P. Taffin de Givenchy, T. Darmanin, O. Choulet, F. Guittard, Green Chem. 15 (2013) 283.

[4] M. Pagliaro, R. Ciriminna, H. Kimura, M. Rossi, C.D. Pina, Angew. Chem. Int. Ed. 46 (2007) 4434-4440.

[5] J.R. Ochoa-Gómez, O. Gómez-Jiménez-Aberasturi, C. Ramírez-López, M. Belsué, Org. Process Res. Dev. 16 (2012) 389-399.

[6] P. Liu, M. Derchi, E.J.M. Hensen, Appl. Catal. B 144 (2014) 135-143.

[7] G. Parameswaram, M. Srinivas, B. Hari Babu, P.S. Sai Prasad, N. Lingaiah, Catal. Sci. Technol. 3 (2013) 3242.

[8] M.G. Álvarez, M. Plíšková, A.M. Segarra, F. Medina, F. Figueras, Appl. Catal. B 113-114 (2012) 212-220.

[9] M.J. Climent, A. Corma, P.D. Frutos, S. Iborra, M. Noy, A. Velty, P. Concepción, J. Catal. 269 (2010) 140-149.

[10] M. Aresta, A. Dibenedetto, F. Nocito, C. Ferragina, J. Catal. 268 (2009) 106-114.

[11] F. Rubio-Marcos, V. Calvino-Casilda, M.A. Bañares, J.F. Fernandez, J. Catal. 275 (2010) 288-293.

[12] S.-i. Fujita, Y. Yamanishi, M. Arai, J. Catal. 297 (2013) 137-141.

[13] J. Li, T. Wang, Chem. Eng. Process. 49 (2010) 530-535.

[14] C. Vieville, J.W. Yoo, S. Pelet, Z. Mouloungui, Catal. Lett. 56 (1998) 245-247.
[15] M. Aresta, A. Dibenedetto, F. Nocito, C. Pastore, J. Mol. Catal. A: Chem. 257 (2006) 149-153.
[16] J. George, Y. Patel, S.M. Pillai, P. Munshi, J. Mol. Catal. A: Chem. 304 (2009) 1-7.
[17] A. Dibenedetto, A. Angelini, M. Aresta, J. Ethiraj, C. Fragale, F. Nocito, Tetrahedron 67 (2011) 1308-1313.
[18] J. Li, T. Wang, J. Chem. Thermodynamics 43 (2011) 731-736.
[19] K. Tomishige, H. Yasuda, Y. Yoshida, M. Nurunnabi, B. Li, K. Kunimori, Green Chem. 6 (2004) 206.
[20] H. Li, D. Gao, P. Gao, F. Wang, N. Zhao, F. Xiao, W. Wei, Y. Sun, Catal. Sci. Technol. 3 (2013) 2801.
[21] J. Zhang, D. He, J. Colloid Interface Sci. 419 (2014) 31-38.
[22] F. Prinetto, G. Ghiotti, J. Phys. Chem. B 104 (2000) 11117-11126.
[23] A. Takagaki, K. Iwatani, S. Nishimura, K. Ebitani, Green Chem. 12 (2010) 578.
[24] M. Malyaadri, K. Jagadeeswaraiah, P.S.S. Prasad, N. Lingaiah, Appl. Catal. A: General 401 (2011) 153-157.
[25] M.G. Álvarez, R.J. Chimentão, F. Figueras, F. Medina, Appl. Clay Sci. 58 (2012) 16-24.
[26] G. Wu, X. Wang, W. Wei, Y. Sun, Appl. Catal. A: General 377 (2010) 107-113.
[27] J.T. Kloprogge, L. Hickey, R.L. Frost, J. Solid State Chem. 177 (2004) 4047-4057.
[28] P. Benito, I. Guinea, F.M. Labajos, J. Rocha, V. Rives, Microporous Mesoporous Mater. 110 (2008) 292-302.
[29] Q. Ma, T. Zhao, D. Wang, W. Niu, P. Lv, N. Tsubaki, Appl. Catal. A: General 464-465 (2013) 142-148.
[30] D.G. Costa, A.B. Rocha, W.F. Souza, S.S.X. Chiaro, A.A. Leitão, Appl. Clay Sci. 56 (2011) 16-22.
[31] X. Fan, Z. Yang, X. Xie, W. Long, R. Wang, Z. Hou, J. Power Sources 241 (2013) 404-409.
[32] Z. Ni, A. Chen, C. Fang, L. Wang, W. Yu, J. Phys. Chem. Solids 70 (2009) 632-638.
[33] E. Lima, J. Martinez-Ortiz Mde, R.I. Gutierrez Reyes, M. Vera, Inorg. Chem. 51 (2012) 7774-7781.
[34] L. Wang, Y. Ma, Y. Wang, S. Liu, Y. Deng, Catal. Commun. 12 (2011) 1458-1462.
[35] B.E. Prasad, P.V. Kamath, K. Vijayamohanan, Langmuir 27 (2011) 13539-13543.
[36] P. Gao, F. Li, H. Zhan, N. Zhao, F. Xiao, W. Wei, L. Zhong, H. Wang, Y. Sun, J. Catal. 298 (2013) 51-60.
[37] P. Gao, F. Li, H. Zhan, N. Zhao, F. Xiao, W. Wei, L. Zhong, Y. Sun, Catal. Commun. 50 (2014) 78-82.
[38] K. Sutthiumporn, S. Kawi, Int. J. Hydrogen Energy 36 (2011) 14435-14446.
[39] L. Jin, Y. Zhang, J.P. Dombrowski, C.-H. Chen, A. Pravatas, L. Xu, C. Perkins, S.L. Suib, Appl. Catal. B 103 (2011) 200-205.
[40] M. Rezayat, H.S. Ghaziaskar, Green Chem. 11 (2009) 710.
[41] I. Dosuna-Rodríguez, E.M. Gaigneaux, Catal. Today 195 (2012) 14-21.
[42] S. Huang, J. Ma, N. Zhao, M. Dong, W. Wei, Y. Sun, Petrochemical Technology 36 (2007) 248-251.
[43] S. Huang, J. Ma, J. Li, N. Zhao, W. Wei, Y. Sun, Catal. Commun. 9 (2008) 276-280.
[44] S. Huang, S. Liu, J. Li, N. Zhao, W. Wei, Y. Sun, Catal. Lett. 118 (2007) 290-294.

[45] J.-H. Park, J.S. Choi, S.K. Woo, S.D. Lee, M. Cheong, H.S. Kim, H. Lee, Appl. Catal. A 433-434 (2012) 35-40.
[46] H. Li, X. Jiao, L. Li, N. Zhao, F. Xiao, W. Wei, Y. Sun, B. Zhang, Catal. Sci. Technol. 5 (2015) 989-1005.

Captions of the illustration

Fig. 1. XRD patterns of prepared HT and HT-X hydrotalcites. *: ZnO, ◊: $La_2(CO_3)_2(OH)_2 \cdot H_2O$ (46-0368), □: La_2CO_5 (23-0320), o: $La_2O_2CO_3$ (37-0804).

Fig. 2. FT-IR spectra of prepared HT and HT-X hydrotalcites.

Fig. 3. SEM images of HT, HT-F, HT-Cl and HT-Br samples.

Fig. 4. TG-DTG curves of prepared HT and HT-X hydrotalcites.

Fig. 5. XRD patterns of calcined catalysts. *: ZnO, o: $La_2O_2CO_3$ (37-0804), ♦: $La_2O_2CO_3$ (48-1113), ∇: LaOF (05-0470), Δ: LaOCl (34-1494).

Fig. 6. SEM images of calcined samples.

Fig. 7. The CO_2-TPD profiles of CHT and CHT-X catalysts. The values of the peak (β, γ and δ) area of CHT, CHT-F, CHT-Cl and CHT-Br were multiplied by 10^{10} and the results are 3.019, 1.311, 1.100 and 1.469 (a.u.)/g, respectively.

Table 1

Weight loss of the prepared HT and HT-X hydrotalcites.

Table 2

Physical properties of CHT and CHT-X catalysts.

Table 3

The binding energies and surface composition of the calcined samples.

Table 4

The catalytic activities of various catalysts for the synthesis of GC.

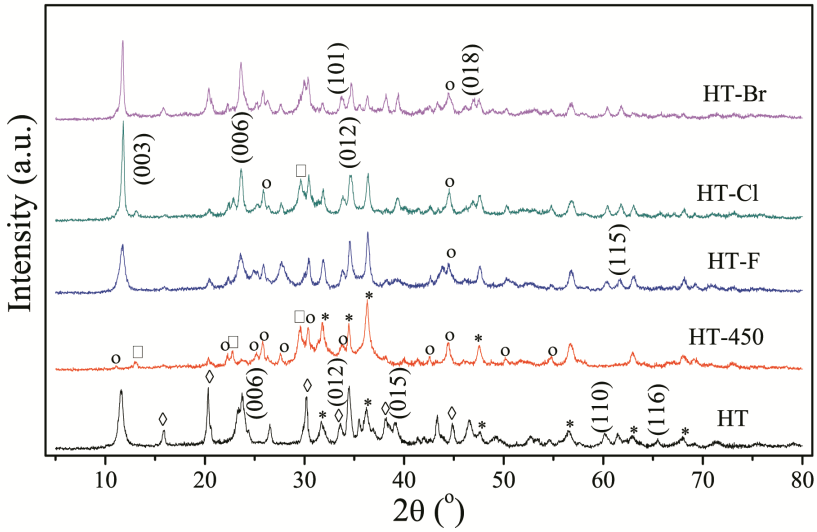

Fig. 1. XRD patterns of prepared HT and HT-X hydrotalcites. *: ZnO, ◊: $La_2(CO_3)_2(OH)_2 \cdot H_2O$ (46-0368), □: La_2CO_5 (23-0320), o: $La_2O_2CO_3$ (37-0804).

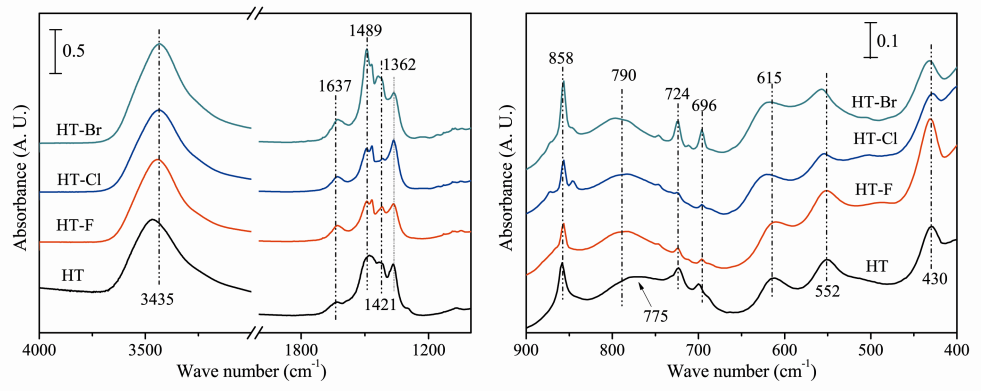

Fig. 2. FT-IR spectra of prepared HT and HT-X hydrotalcites.

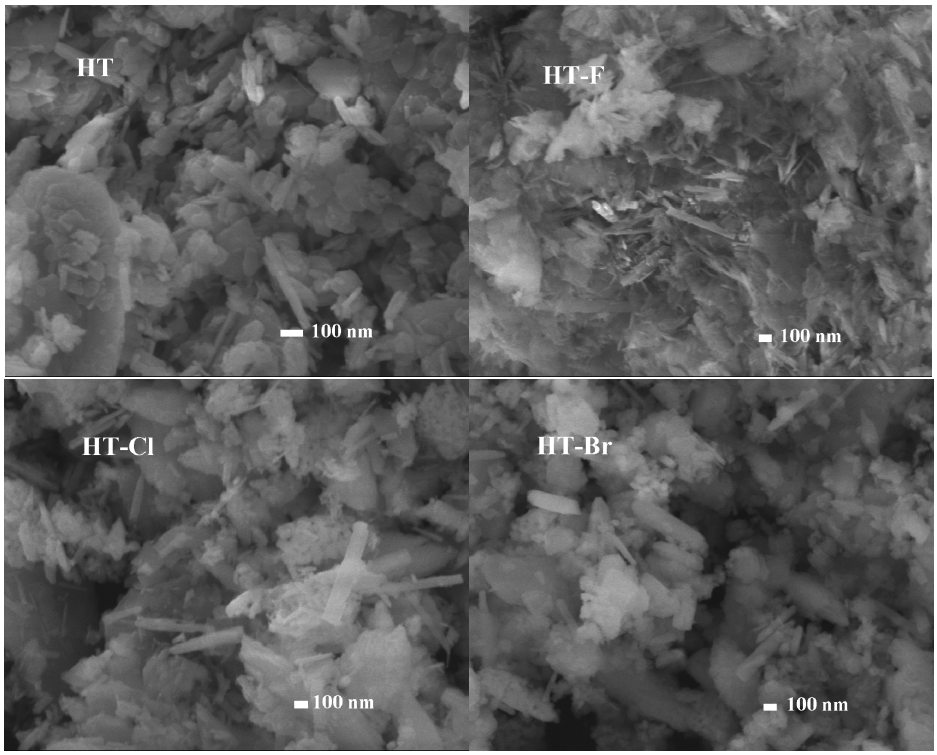

Fig. 3. SEM images of HT, HT-F, HT-Cl and HT-Br samples.

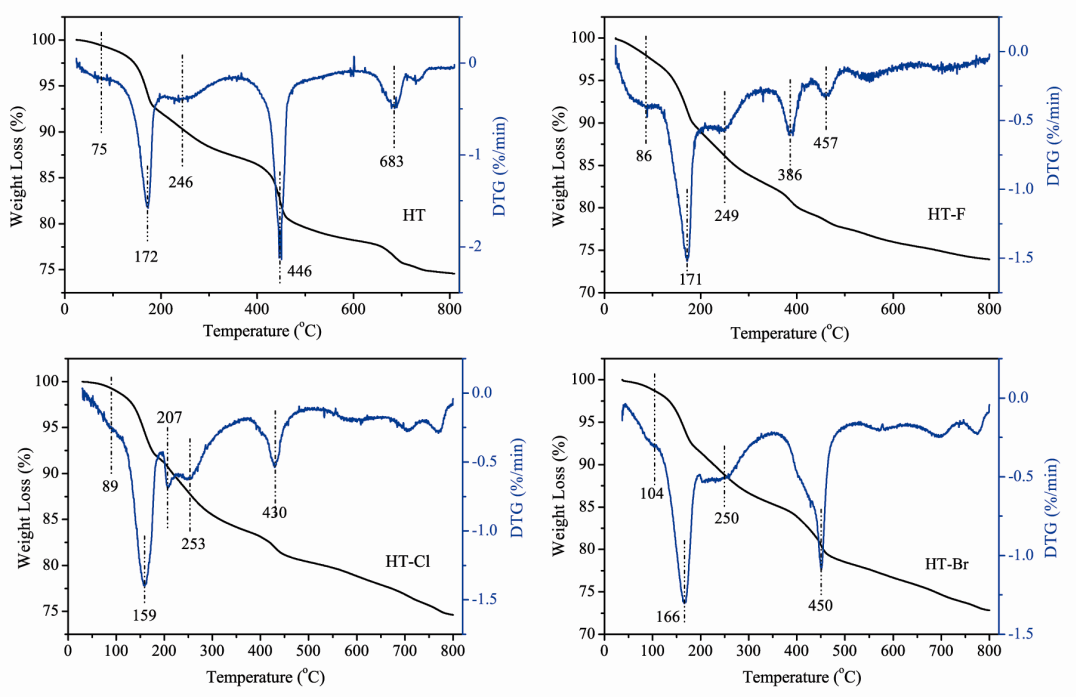

Fig. 4. TG-DTG curves of prepared HT and HT-X hydrotalcites.

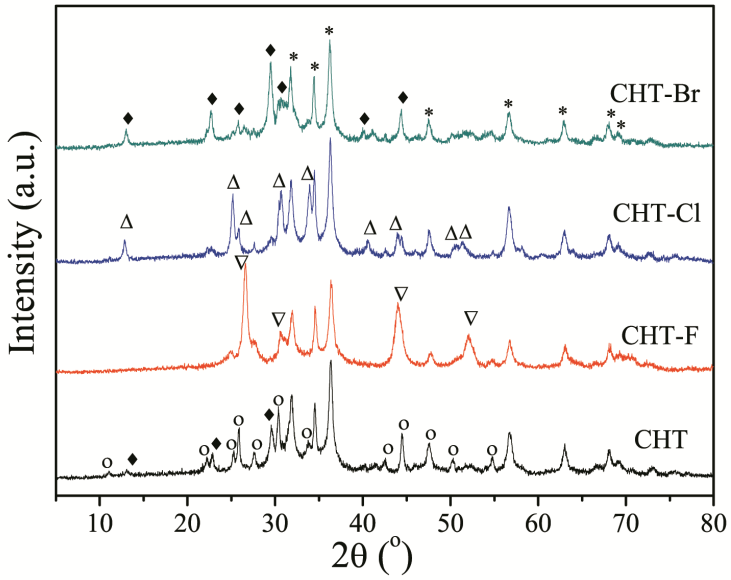

Fig. 5. XRD patterns of calcined prepared catalysts. *: ZnO, o: $La_2O_2CO_3$ (37-0804), ♦: $La_2O_2CO_3$ (48-1113), ∇: LaOF (05-0470), Δ: LaOCl (34-1494).

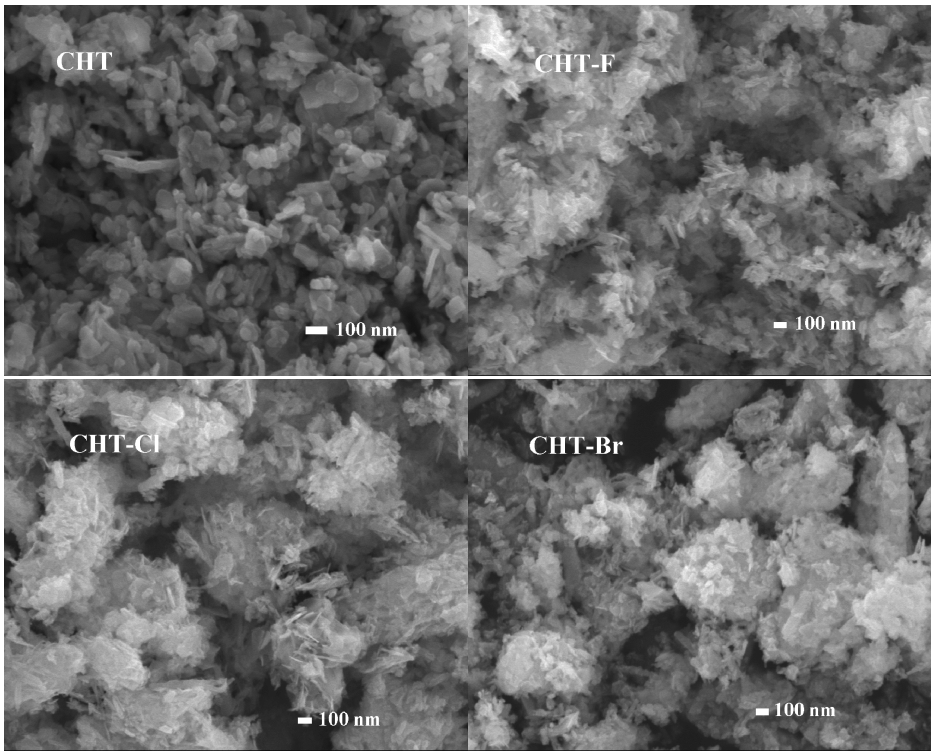

Fig. 6. SEM images of calcined samples.

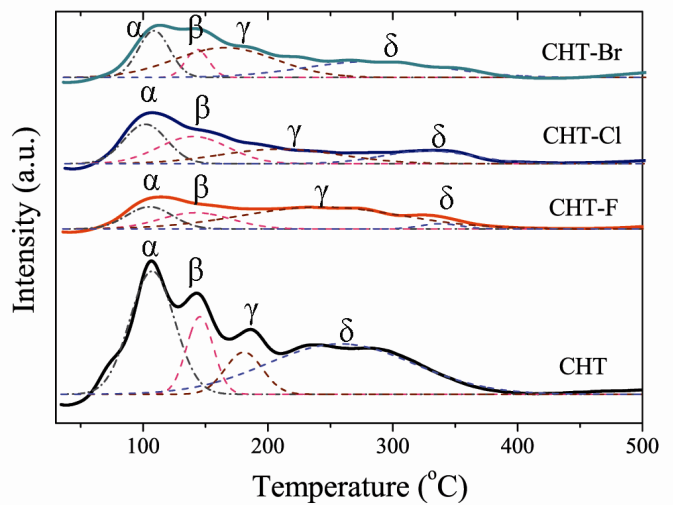

Fig. 7. The CO_2-TPD profiles of CHT and CHT-X catalysts. The values of the peak (β, γ and δ) area of CHT, CHT-F, CHT-Cl and CHT-Br were multiplied by 10^{10} and the results are 3.019, 1.311, 1.100 and 1.469 (a.u.)/g, respectively.

Table 1. Weight loss of the prepared HT and HT-X hydrotalcites.

Samples	Weight Loss (%)*		
	First (< 200 ^{o}C)	Second (200-300 ^{o}C)	Third (300-500 ^{o}C)
HT	7.5	5.0	8.7
HT-F	11.1	5.8	5.6
HT-Cl	8.6	7.6	3.8
HT-Br	8.3	6.5	7.2

*Obtained from the TG-DTG curves of Fig. 4.

Table 2. Physical properties of CHT and CHT-X catalysts.

Sample	Surface area (m^2/g)	Pore volume (cm^3/g)	Pore radius (nm)
CHT	36.4	0.069	5.6
CHT-F	46.2	0.13	6.6
CHT-Cl	53.1	0.20	8.1
CHT-Br	61.4	0.16	5.3

Table 3. The binding energies and surface composition of calcined samples.

Samples	Binding Energy (eV)				Surface percentage (at.%)			
	Zn	La	Al	X	Zn	La	Al	X
CHT	1020.8	834.4	74.6	-	17.9	4.4	3.8	-
CHT-F	1021.3	835.3	74.3	684.9	26.1	2.5	6.2	4.8
CHT-Cl	1021.1	835.0	74.5	199.2	23.6	2.7	6.8	2.8
CHT-Br	1021.0	834.8	74.1	69.2	22.7	4.1	6.2	0.9

X represents F, Cl and Br in CHT-F, CHT-Cl and CHT-Br, respectively.

Table 4. The catalytic activities of various catalysts for the synthesis of GC.

Sample	Glycerol Conversion (%)	Selectivity (%)			GC Yield (%)
		Monoacetin	Diacetin	GC	
CHT	30.4	50.9	5.2	43.8	13.3
CHT-F	30.6	46.9	7.0	46.1	14.1
CHT-Cl	35.5	47.0	7.7	45.2	16.0
CHT-Br	33.6	48.9	6.8	44.2	14.8
Used CHT-Cl	26.9	44.8	2.8	52.3	14.0

Reaction condition: Glycerol 4.60 g, CH_3CN 5.0 mL, catalyst 0.14 g, Initial pressure P_{CO2}=4.0 MPa, 170 ^{o}C, 12 h.